The use of helical spring and fluid damper isolation systems for bridge structures subjected to vertical ground acceleration

A. Parvin [1] and **Z. Ma** [2]

[1] *A/Professor, Department of Civil Engineering, University of Toledo, OH 43606-3390 USA*
Email: aparvin@eng.utoledo.edu
[2] *Former Grad. Student, Department of Civil Engineering, University of Toledo, OH 43606-3390 USA*

Received 17 May 2001; revised 22 July 2001; accepted 24 July 2001

ABSTRACT

In this study a combination of helical springs and fluid dampers are proposed as isolation and energy dissipation devices for bridges subjected to earthquake loads. Vertical helical springs are placed between the superstructure and substructure as bearings and isolation devices to support the bridge and to eliminate or minimize the damage due to earthquake loads. Additionally, horizontal helical springs are placed between the abutments and bridge deck to save the structure from damage. Since helical springs provide stiffness in any direction, a multi-directional seismic isolation system is achieved which includes isolation in the vertical direction. To reduce the response of displacement, nonlinear fluid dampers are introduced as energy dissipation devices. Time history analysis studies conducted show that the proposed bridge system is sufficiently flexible to reduce the response of acceleration. The response of displacement due to provided flexibility is effectively controlled by the addition of energy dissipation devices.

KEYWORDS

Seismic isolated structures; dynamic analysis; vertical motion; helical spring.

1. Introduction

Seismic isolation reduces the response of a structure during an earthquake by introducing flexibility and energy dissipation capabilities. Generally, horizontal inertia forces cause the most damage to a structure during an earthquake. Since the magnitude of the vertical ground acceleration component is usually less than the horizontal ground acceleration component, vertical seismic loads are not considered in the design of most structures. The vertical acceleration is typically taken as two thirds of the horizontal acceleration component for the same response spectral curve.

However, recent observation and analysis of earthquake ground motion have shown that the vertical motion in bridges should not be completely ignored. Researchers compiled records and photographs of damage and failures of buildings and bridges due to high vertical motion. Ratios of peak vertical-to-horizontal acceleration have been recorded as high as 1.6, while the conventional design assumption is 0.67 [1]. Damage from Kalamata, Greece (1986), Northridge, CA (1994), and Kobe, Japan (1995) due to purely vertical effects is reported, along with the high vertical -to-horizontal acceleration ratios.

Not many researchers address vertical motion in their studies. Among the few who have, Button et al. [2] investigated the effect of vertical ground acceleration on six bridge types and they recommended criteria for inclusion or exclusion of vertical ground motion in the design and analysis of bridges. Their study was limited to bridges with no base isolation and energy dissipation devices. Waisman and Grigoriu [3] studied the influence of the vertical seismic

component on a friction-pendulum type base-isolated bridge. Their model was limited to a single span, and single degree-of-freedom system. Saadeghvaziri and Foutch [4] investigated the behavior of reinforced concrete highway bridges that were not isolated and were subject to combined vertical and horizontal earthquake motions. They concluded that it is important to include the vertical component of ground acceleration motion in the design of highway bridges.

Most research studies in bridge isolation, where the vertical ground motion is neglected, include theoretical and experimental analysis of various active and passive isolators (for horizontal plane motions) that are not multi-directional and are complex in some cases. Among such recent studies, Xue et al. [5] proposed a new system termed the Intelligent Passive Vibration Control (IPVC), which contains both passive (isolation) and intelligent, or active (damping) elements. During small earthquakes, only the passive system is utilized. During large earthquakes, the active system is triggered by displacement limitations. Further experimental and analytical results on passive/active control of a bridge, which employs sliding bearings with recentering springs for isolation, and servo-hydraulic actuators activated by absolute acceleration records, are reported by Nagarajaiah et al. [6]. This system allows for a sliding system with higher friction to be implemented without fear of high acceleration response. Yang et al. [7] presented analytical models for rubber and sliding bearings coupled with actuators for bridges.

The vertical motion in the bridge is crucial. The uplift from the vertical motion may cause loss of contact followed by impact, which is likely to lead to higher mode response and large axial forces in the piers. Existing bridge bearings including elastomeric bearings and lead rubber bearings among others are designed to only provide isolation in the horizontal plane. For instance, in some cases, using only horizontal isolation may provide sufficient protection against an earthquake. However, in certain other cases, where vertical ground acceleration is significant, a multi-directional isolation system, which possibly employs helical springs may be required.

This study involves novel bridge bearings consisting of helical springs and viscous dampers to achieve a multi-directional seismic isolation system, which also provides controlled flexibility in the vertical direction. In the proposed configuration of the isolated bridge (Fig.1), the deck and girders can be considered to be floating on helical spring bearings. Helical springs, which have both vertical and shear stiffness, are designed to support vertical loads, including the self-weight of the bridge, providing the mechanism to accommodate movement in all directions. To protect the bridge deck and abutment from damage by an earthquake in the longitudinal direction, helical springs are also installed between the deck and abutments. Additionally, fluid dampers are added vertically at the locations of the interface between the superstructure and its supporting pier and abutment to control the response of displacement during an earthquake. The combination of helical springs and fluid dampers is expected to provide an efficient flexible seismic isolation and energy dissipation device that reduces the response of the system.

The following sections discuss the mathematical models for the damper and helical spring of the bridge model. A numerical analysis study for the vertical response of the bridge with the proposed isolation system, is then presented followed by the conclusions.

2. Characterization of elements in proposed isolation system

Two fundamental isolation and energy dissipation elements presented in this section include the helical spring and the fluid damper, respectively. The helical spring possesses stiffness in all directions. Its stiffness can be customized according to design requirements. Compared to a non-isolated bridge, a spring-supported bridge is relatively flexible in the vertical direction, allowing vibration in the vertical direction with no damage to the structure. The helical spring

can greatly reduce the relative response of acceleration. Other advantages of using helical springs include high load carrying capacity, linear load versus deflection curve, nearly unlimited lifetime service (if provided with suitable corrosion protection), and constant properties with time [8]. These combined properties make the helical spring a very suitable elastic element with a restoring force. However, the helical spring has little damping effect [9]. If additional damping is required for practical purposes, supplemental damping devices can be combined with the springs or used separately.

The helical spring follows a linear relationship where elastic force is proportional to relative deformation. The relationship between static force and relative deformation of a helical spring is:

$$F_v = k_v v, \tag{1a}$$

where k_v is the vertical stiffness of spring, and v is the relative deflection in vertical direction. The shear stiffness is taken as 40% ~ 50% of the vertical stiffness [8,10]. In the shear direction, a similar relationship is taken as:

$$F_s = k_s u = \eta k_v u, \tag{1b}$$

where k_s is the shear stiffness of helical spring, u is the relative deflection in shear direction, and η is the ratio coefficient and is equal to $40\% \sim 50\%$. The spring stiffness is linear for static or dynamic analysis, which is a significant simplifying factor for the numerical analysis.

Fluid dampers have been used or proposed for structures as energy dissipation devices during the past three decades. Taylor and Constantinou [11] reported multiple episodes of high capacity fluid damping devices being used in buildings, bridges and related structures, which were originally invented and developed to attenuate the shock and blast effects in military equipment. Constantinou et al. [12] studied the effect of various passive energy dissipation systems used in buildings.

The fluid damping level can be up to 20%~50% of critical, thus greatly decreasing the response of displacement [11,13]. The output force of the fluid damper is insensitive to temperature. This property allows greater versatility in the application of these devices. In addition, there are also noteworthy advantages in installation, operation and maintenance of the fluid dampers and they have been proven to be reliable and cost effective.

The output force of the fluid damper at any time is typically represented as:

$$P = C_d \dot{u}^r, \tag{2}$$

where $\dot{u}$ is the velocity of the piston rod, C_d is the damping coefficient, and r is the exponent coefficient, ranging from 0.1 to 1.8 as manufactured [14]. The piston rod stroke and the damping output force are mechanical characteristics of the fluid damper. The piston rod movement is limited to its stroke. Therefore, the displacement of the damped system should not be greater than the maximum stroke of the fluid damper. The fluid damper can provide damping in its axial direction only. To eliminate the damage caused by non-axial forces to the damper, a roller is placed at the end of the piston rod.

Damping ratio is used as a measure to evaluate the damping level of a multi-mode damped system, and can be obtained for any mode as:

$$\xi_i = \frac{E_{di}}{\pi E_{si}}, \tag{3}$$

where ξ_i is the damping ratio of the *i*th mode, E_{di} is the total energy dissipated by the fluid damper per cycle, and E_{si} is the total elastic energy of the system per cycle for the *i*th mode.

For a structure subjected to dynamic loading, the equivalent damping ratio throughout the complete duration t_0 of the loading is:

$$\xi = \frac{\sum_{j}^{t_0} P_j D_j}{\pi \sum_{j}^{t_0} F_j D_j} \tag{4}$$

where P_j is the damping force, F_j is the elastic force, and D_j is the response of displacement at any jth time step.

Equation (4) will be used in this study as the basic formula to evaluate the damping ratio, which will be an approximation if the forces and displacements are solved numerically. Harmonic motion is a special case of Equation (4). It is noted that for a linear fluid damper, the damping ratio is independent of amplitude of motion. For a non-linear case, the damping ratio generally reduces with increasing amplitude of motion.

Structural system damping is another factor that affects the dynamic performance of the structure. This damping is defined as the resistance to motion provided by the internal friction of the materials. The friction develops as the molecules forming the materials are forced across one another when the structure moves relatively. However, evaluation of system damping cannot be easily performed in practice. Usually, some percentage of critical damping is taken instead [15].

3. Modeling of bridge

For dynamic analysis, the isolated bridge (Fig.1) can be modeled as a continuous beam for simplicity. Since this model is flexible in the vertical direction, it cannot be considered as a rigid block in that direction. The entire vertical load is carried by helical spring bearings. Fluid dampers are placed at the location of the bearings and do not support the vertical load. Their functions are to dissipate seismic energy, suppress possible resonance, and limit displacements. If a group of springs and dampers is employed at one location of the bridge, the resultant stiffness as well as the damping of the springs and dampers need to be calculated for a particular direction. Fluid dampers provide damping in only one direction, while helical springs have stiffness in all directions.

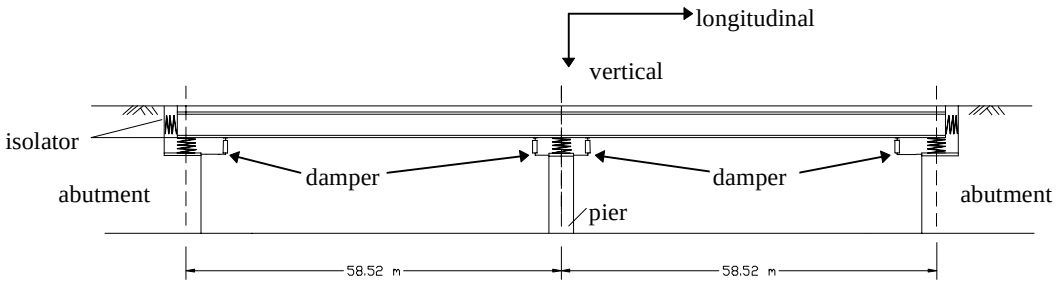

Figure 1. Two-Span Box Girder Bridge Prototype

The displacement method is used to construct the relationship between the force and deformation of a deformable body. The derivation follows the typical procedure of matrix structural analysis for the bridge model [16,17]. In this model, the total stiffness matrix $\mathbf{K_c}$ is found by adding the supporting spring stiffness to the diagonal element of the global stiffness matrix at the corresponding degrees-of-freedom.

A consistent approach for mass accounts for translational, as well as rotational degrees-of-freedom, while the lumped mass approach only considers the translational degrees-of-freedom. Since the rotational component of earthquake ground motion is not considered in most cases, the motion in rotational degrees-of-freedom would not be excited. Additionally, in the lumped mass bridge model, the amount of rotations compared to translations are insignificant. Hence, the rotational degrees-of-freedom are excluded from the stiffness matrix.

The static stiffness equation, which is $\mathbf{F} = \mathbf{K}_c \Delta$ in matrix form, is partitioned as:

$$\begin{bmatrix} \mathbf{K}_{vv} & \mathbf{K}_{v\theta} \\ \mathbf{K}_{\theta v} & \mathbf{K}_{\theta\theta} \end{bmatrix} \begin{Bmatrix} \mathbf{v} \\ \theta \end{Bmatrix} = \begin{Bmatrix} \mathbf{F}_v \\ \mathbf{F}_\theta \end{Bmatrix}, \tag{5}$$

where $\mathbf{v}$ and θ represent translation and rotation, respectively.

If $\mathbf{F}_\theta = \mathbf{0}$ in Equation (5), then $\theta = -\mathbf{K}_{\theta\theta}^{-1} K_{\theta v} \mathbf{v}$. Substituting into the first submatrix in Equation (5) yields:

$$(\mathbf{K}_{vv} - \mathbf{K}_{v\theta} \mathbf{K}_{\theta\theta}^{-1} \mathbf{K}_{\theta v}) \mathbf{v} = \mathbf{F}_v \text{ or } \mathbf{K}\mathbf{v} = \mathbf{F}_v, \tag{6}$$

where $\mathbf{K} = \mathbf{K}_{vv} - \mathbf{K}_{v\theta} \mathbf{K}_{\theta\theta}^{-1} \mathbf{K}_{\theta v}$ is the translation stiffness matrix. Only those degrees-of-freedom related to translation are retained. Therefore, the condensed matrix becomes compatible for use with the diagonal lumped mass matrix **M**.

The system damping matrix is expressed as:

$$\mathbf{C}_s = (\mathbf{M}\phi[\phi^T \mathbf{M}\phi]^{-1}) \mathbf{c}_m ([\phi^T \mathbf{M}\phi]^{-1} \phi^T \mathbf{M}), \tag{7}$$

where ϕ is the modal shape matrix and $\mathbf{c}_m$ is the generalized modal damping matrix.

The diagonal damping matrix when fluid dampers are placed at the bearings in the vertical direction is represented by $\mathbf{C}_d$. The damping forces of fluid dampers are determined by the damping coefficient, the damping exponent, and the velocity of the piston.

The dynamic equation of the base-isolated bridge model in the vertical direction has the following nonlinear form:

$$\mathbf{M}\ddot{\mathbf{W}} + \mathbf{C}_s \dot{\mathbf{W}} + \mathbf{C}_d \dot{\mathbf{W}}^r + \mathbf{K}\mathbf{W} = -\mathbf{M}\ddot{\mathbf{W}}_g, \tag{8}$$

where $\ddot{\mathbf{W}}_g$ is the acceleration of the earthquake ground motion, $\mathbf{W}, \dot{\mathbf{W}}, \ddot{\mathbf{W}}$ are the vector of vertical displacement, velocity and acceleration, respectively.

Among numerous direct integration methods to solve for the nonlinear response in Equation (8), the Newmark integration method appears to be the most effective with the smallest numerical errors. In the Newmark method, the acceleration is assumed to be linear for the time t to $t + \Delta t$. For the time interval Δt, following relations are assumed:

$$\dot{\mathbf{W}}_{t+\Delta t} = \dot{\mathbf{W}}_t + [(1-\beta)\ddot{\mathbf{W}}_t + \beta\ddot{\mathbf{W}}_{t+\Delta t}]\Delta t \text{ and} \tag{9a}$$

$$\mathbf{W}_{t+\Delta t} = \mathbf{W}_t + \dot{\mathbf{W}}_t \Delta t + [(\tfrac{1}{2} - \alpha)\ddot{\mathbf{W}}_t + \alpha\ddot{\mathbf{W}}_{t+\Delta t}]\Delta t^2, \tag{9b}$$

where α and β are parameters used to achieve the integration accuracy and stability. In the case of $\alpha = \frac{1}{4}$ and $\beta = \frac{1}{2}$, the constant-average-acceleration method will yield unconditional stability in the iteration procedure.

From Equations (9a) and (9b), $\dot{\mathbf{W}}_{t+\Delta t}$ and $\ddot{\mathbf{W}}_{t+\Delta t}$ can be solved in terms of $\mathbf{W}_{t+\Delta t}$ as follows:

$$\ddot{\mathbf{W}}_{t+\Delta t} = \frac{1}{\alpha \Delta t^2}(\mathbf{W}_{t+\Delta t} - \mathbf{W}_t) - \frac{1}{\alpha \Delta t}\dot{\mathbf{W}}_t - (\frac{1}{2\alpha} - 1)\ddot{\mathbf{W}}_t \text{ and} \tag{10a}$$

$$\dot{\mathbf{W}}_{t+\Delta t} = \dot{\mathbf{W}}_t + \Delta t(1-\beta)\ddot{\mathbf{W}}_t + \beta \Delta t \ddot{\mathbf{W}}_{t+\Delta t}. \tag{10b}$$

To obtain the solution for displacement, velocity and acceleration at time $t + \Delta t$, the equilibrium Equation (8) is rewritten as:

$$\mathbf{M}\ddot{\mathbf{W}}_{t+\Delta t} + \mathbf{C_s}\dot{\mathbf{W}}_{t+\Delta t} + \mathbf{C_d}\dot{\mathbf{W}}^r_{t+\Delta t} + \mathbf{K}\mathbf{W}_{t+\Delta t} = -\mathbf{M}(\ddot{\mathbf{W}}_{\mathbf{g}})_{t+\Delta t}. \tag{11}$$

Since $\mathbf{C_d}\dot{\mathbf{W}}^r_{t+\Delta t}$ is a nonlinear term, substituting Equations [10a] and [10b] into Equation [11] will not yield linear simultaneous equations with respect to $\mathbf{W}_{t+\Delta t}$. Hence $\mathbf{W}_{t+\Delta t}$ cannot be solved directly. To avoid using the iteration technique to solve the displacement vector at each time step, the nonlinear term $\dot{\mathbf{W}}^r_{t+\Delta t}$ is expanded at time t by a Taylor series as shown in the following equation:

$$\dot{\mathbf{W}}^r_{t+\Delta t} = \dot{\mathbf{W}}^r_t + r \cdot diag(\dot{\mathbf{W}}^{r-1}_t)(\dot{\mathbf{W}}_{t+\Delta t} - \dot{\mathbf{W}}_t), \tag{12}$$

where it is assumed that the high order terms can be neglected without loss of acceptable accuracy and $diag$ is an operator to diagonalize a vector to a matrix.

By substituting Equations (10a), (10b), and (12) in Equation (11), a linear equation with respect to $\mathbf{W}_{t+\Delta t}$ at each time step is obtained as:

$$\tilde{\mathbf{K}}\mathbf{W}_{t+\Delta t} = \tilde{\mathbf{P}}_{t+\Delta t}, \tag{13}$$

$$\tilde{\mathbf{K}} = \mathbf{K} + \frac{1}{\alpha \Delta t^2}\mathbf{M} + \frac{\beta}{\alpha \Delta t}\mathbf{C_m} + \frac{r\beta}{\alpha \Delta t}\mathbf{C_d} diag(\dot{\mathbf{W}}^{r-1}_t),$$

$$\tilde{\mathbf{P}}_{t+\Delta t} = -\mathbf{M}(\ddot{\mathbf{W}}_{\mathbf{g}})_{t+\Delta t} + \mathbf{M}\mathbf{a_M} + \mathbf{C_s}\mathbf{a}_{\mathbf{C_s}} + \mathbf{C_d}\mathbf{a}_{\mathbf{C_d}},$$

$$\mathbf{a_M} = \frac{1}{\alpha \Delta t^2}\mathbf{W}_t + \frac{1}{\alpha \Delta t}\dot{\mathbf{W}}_t + (\frac{1}{2\alpha} - 1)\ddot{\mathbf{W}}_t,$$

$$\mathbf{a}_{\mathbf{C_s}} = \frac{\beta}{\alpha \Delta t}\mathbf{W}_t + (\frac{\beta}{\alpha} - 1)\dot{\mathbf{W}}_t + \Delta t(\frac{\beta}{2\alpha} - 1)\ddot{\mathbf{W}}_t, \text{ and}$$

$$\mathbf{a}_{\mathbf{C_d}} = \frac{\beta}{\alpha \Delta t}\mathbf{W}_t - \dot{\mathbf{W}}^r_t + \frac{r\beta}{\alpha} diag(\dot{\mathbf{W}}^{r-1}_t)\dot{\mathbf{W}}_t + \beta \Delta t(\frac{1}{2\alpha} - 1)\ddot{\mathbf{W}}_t - r\Delta t(1-\beta) diag(\dot{\mathbf{W}}^{r-1}_t)\ddot{\mathbf{W}}_t.$$

After $\mathbf{W}_{t+\Delta t}$ is solved from Equation (13), $\ddot{\mathbf{W}}_{t+\Delta t}$ and $\dot{\mathbf{W}}_{t+\Delta t}$ can be obtained from Equations (10a) and (10b), respectively. Since the velocity and acceleration at time $t + \Delta t$ have been expressed in terms of their previous values at time t after the displacement at time $t + \Delta t$ is known, the iteration procedure can be performed step-by-step with any given initial conditions.

In the above analysis, it can be shown that the nonlinear problem has been simplified to be an approximately linear problem by employing a Taylor series expansion to the nonlinear term of the damping force at each time step. Next the displacements at each time step are solved directly, and therefore the step-by-step direct integration method can be implemented.

4. Description of the proposed bridge model

A flexible system will be less susceptible to damage when subjected to an earthquake excitation. However, there is concern over the issue of isolation for an ideally flexible system. In practice, the bridges need to be designed with sufficient amount of strength and stiffness to resist the service load. The basic factors including the spring stiffness involved in engineering design are taken into consideration for the two-span bridge model in this study. The span length

is based on the continuous beam model. Once the span length is decided, the size of the cross section can be calculated by applying traffic load as a live load plus the dead load of the bridge model, assuming the material is concrete. Note that the deflection under normal bridge loading must be controlled and can be the determinant for the bridge stiffness. From the point of seismic isolation, the bearings are expected to be as flexible as possible. Since the large displacement due to flexibility can be effectively reduced by fluid dampers, the spring stiffness will be mainly determined by operational loading. The stiffness of the springs can be calculated based on the reaction at the bearing and the static settlement limit (fluid dampers are not accounted for carrying the load). Also the kinetic deflection change between traffic load on and off the bridge should be considered as a factor to determine the spring stiffness.

Based on the above analysis, a two-span continuous concrete slab and box girder bridge illustrated in Fig.1 is employed as a model to demonstrate the isolation effects of helical springs and fluid damper systems. This bridge is supported and isolated by helical springs positioned in the vertical direction as bearings. Helical springs are also installed longitudinally at both ends between the abutment and the deck to protect the bridge from impact load. Fluid dampers are located between the superstructure and substructure in the vertical direction where necessary. The length of the bridge model is 58.5 m (192 ft) for each span. AASHTO HS20-44 truck loading is used for the live load. The dead weight of the bridge superstructure is estimated to be 2.138×10^4 kg/m (14.357 kip/ft). The typical cross-section of the bridge box girder has a width of 12.95m (42.5 ft) and a height of 2.36 m (7.75 ft). The moment of inertia in the vertical direction is 66.4 m^4 (1.594×10^8 in^4). Under the presumed total load, the maximum deflection of the bridge is approximately 100 mm (4 in), and the deflection change between traffic on and off the bridge is limited to less than 6 mm (0.24 in). The stiffness of the helical springs is defined by the following, where the shear stiffness is assumed to be 40% of the vertical stiffness:

Vertical stiffness of the spring placed at end bearing $4.9 \times 10^4\ kN/m$ (32. 905 $kip/\ ft$).

Vertical stiffness of spring placed at the middle bearing is $14.7 \times 10^4\ kN/m$ (98.716 $kip/\ ft$).

Vertical stiffness of the spring placed at the abutment is $10^3\ kN/m$ (0. 672 $kip/\ ft$).

Fig.2 illustrates this two-span bridge, which is simplified as a five-lumped-mass model when analyzed numerically. The appropriate damping force relation, in accordance with the manufacturer provided data for the damper, is selected as (Fig.3)

$$P = 1000V^{0.75} \tag{14}$$

where V is the velocity of the piston rod [18]. Fig.4 gives the diagram of the damping force-displacement relationship for the case of harmonic motion with period π and 2π. The enclosed loop areas are the total energies that can be dissipated by the damper in one cycle of harmonic motion. For different periods, the damper has a different area. When the system is subjected to the earthquake motion, the loops will not be symmetrical shapes. However, the energy dissipation capability indicated by the diagram could be useful in selecting the parameters for the fluid damper.

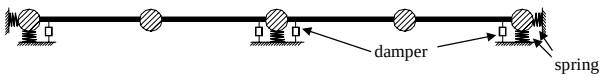

Figure 2. Lumped Mass Bridge Model

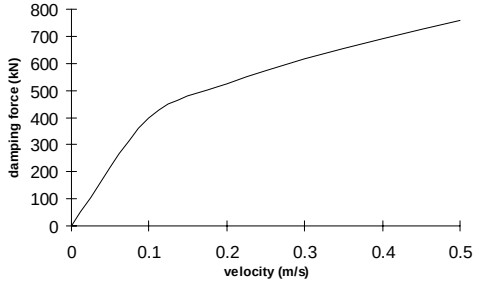

Figure 3. Damping Force-Velocity Relationship of Selected Fluid Damper

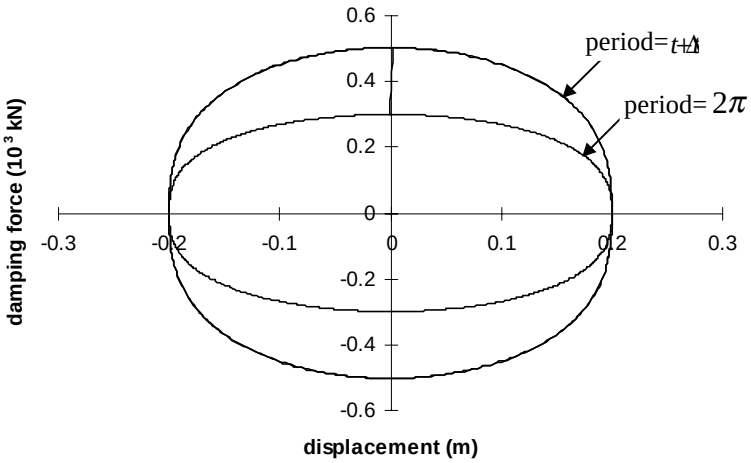

Figure 4. Harmonic Damping Force-Displacement Relationship

5. Vertical response of the bridge

Among the software tools to perform the required numerical analysis for structures with protective devices against earthquakes, the 3-D BASIS by Nagarajaiah et al. [19] is noteworthy. This tool has the capability to analyze various hybrid isolation configurations for three-dimensional seismic motion. Although this numerical analysis software covers modeling of various combinations of isolators and energy dissipation devices, it assumes the isolation devices are rigid in the vertical direction. This model of isolation devices is more applicable for approximation of elastomeric bearing behavior, which is almost incompressible, and has large vertical stiffness, while the shear stiffness is not more than one percent of the vertical stiffness.

In our study, the MATLAB^{TM} software package is employed to obtain the responses of the bridge model illustrated in Fig.1. The bridge is subjected to the vertical components of the Northridge and El Centro earthquakes. Initially, isolated systems with various damping ratios are considered to observe the effect of damping level on the system. During the next step, vertical response of the isolated and undamped, isolated and damped, and non-isolated bridge models are compared to observe the isolation effect of coil springs in the bridge model with or without dampers.

In the bridge model, the natural frequency of the first mode in the vertical direction is 1.56 Hz . The Northridge vertical ground motion, with peak acceleration of 0.799 g , and El Centro vertical ground motion with peak acceleration of 0.210 g are used as input excitations (Fig. 5). The system damping ratio is assumed to be two percent of the critical.

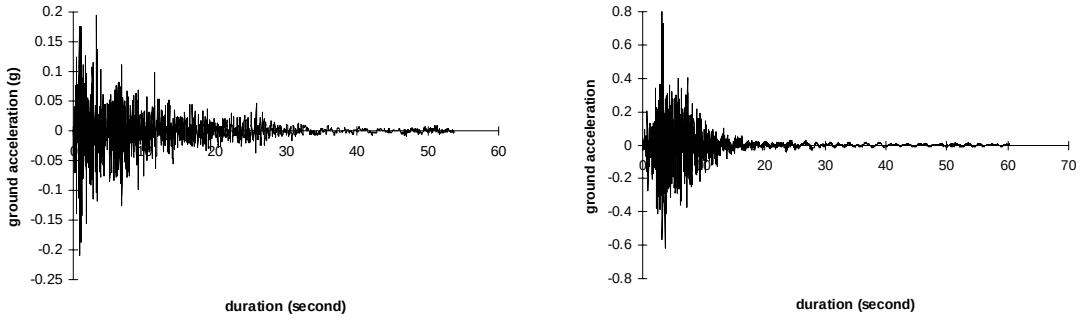

(a) El Centro (b) Northridge

Figure 5. Vertical Ground Accelerations

Initially, the effect of fluid dampers placed at the bridge bearing on the vertical response of the isolated bridge system was studied. Maximum responses and damping level of all the undamped and damped cases for Northridge and El Centro earthquakes are compared in Table 1. For the Northridge earthquake, the undamped responses at mid-span of the bridge model are illustrated in Fig.6. The maximum response of acceleration at mid-span is $0.796\,g$ and the dynamic deflection is over $78\,mm$ $(3\,in)$. To reduce the displacement response, fluid dampers are used for the bridge model. For the damped case with one fluid damper placed at each bearing, responses of the bridge model are shown in Fig.7. The maximum response of mid-span displacement in the damped case reduces 40.5% from $78.6\,mm\,(3\,in)$ to $46.\,mm\,(1.84\,in)$ of the undamped case. The maximum response of mid-span velocity and acceleration also decreases 23.7% and 34.3%, respectively, when the fluid damping level is 9.16%. Fluid dampers exhibit excellent damping effects for the bridge model. The damping force versus displacement loop of the damper at the middle bearing is illustrated in Fig.8. Unlike the curves in Fig.3, the shape of the loop is not symmetric. The acceleration versus displacement hysteresis of the lumped mass at mid-span of damped case bridge model is shown in Fig. 9. The maximum response of displacement is reduced to $46.8\,mm$ $(1.84\,in)$ and the maximum response of acceleration is also as small as $0.523\,g$.

Table 1 Maximum Vertical Responses of the Bridge Model

Earthquake	Location	Damping	Displacement (mm)	Velocity (mm/s)	Acceleration (g)	Fluid Damping (%)
Northridge		Undamped	76.3	700.4	0.749	0
	End bearing	1 damper	44.8	521.6	0.503	9.16
		2 dampers	32.3	432.4	0.463	19.35
		Undamped	78.6	727.9	0.796	0
	Mid-span	1 damper	46.8	555.3	0.523	9.16
		2 dampers	36.1	504.7	0.473	19.35
		Undamped	75.9	696.6	0.748	0
	Center bearing	1 damper	45.2	546.0	0.541	9.16
		2 dampers	36.5	515.0	0.603	19.35
El Centro		Undamped	23.0	233.1	0.225	0
	End bearing	1 damper	10.7	109.0	0.128	13.30
		2 dampers	7.6	75.5	0.115	28.36
		Undamped	23.7	239.5	0.240	0
	Mid-span	1 damper	11.9	118.0	0.139	13.30
		2 dampers	9.0	101.5	0. 153	28.36
		Undamped	22.8	233.1	0.223	0
	Center bearing	1 damper	11.9	120.3	0.147	13.30
		2 dampers	9.3	96.0	0.163	28.36

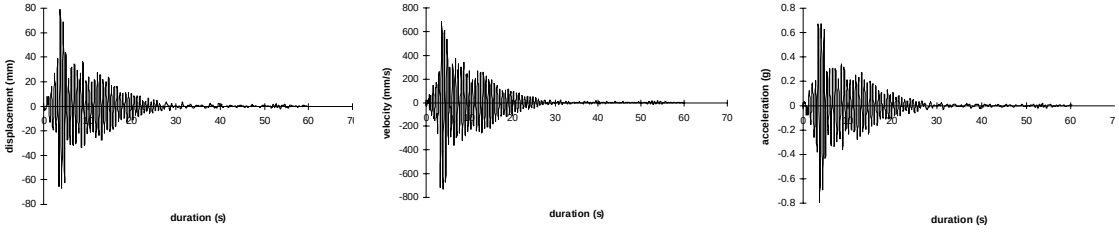

(a) (b) (c)

Figure 6. (a) Displacement; (b) Velocity; (c) Acceleration Responses at Mid-Span (Northridge, Undamped)

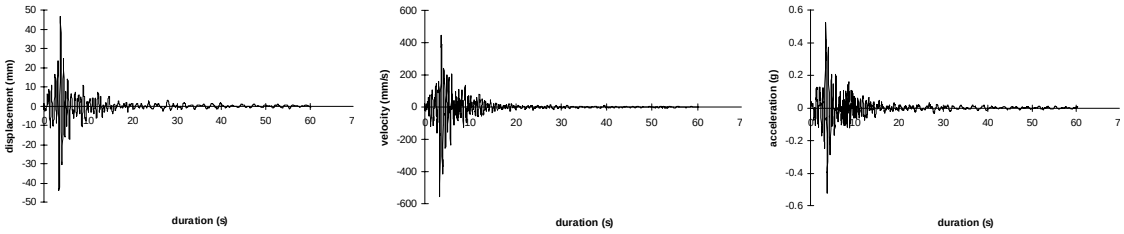

(a) (b) (c)

Figure 7. (a) Displacement; (b) Velocity; (c) Acceleration Responses at Mid-Span (Northridge, Damped)

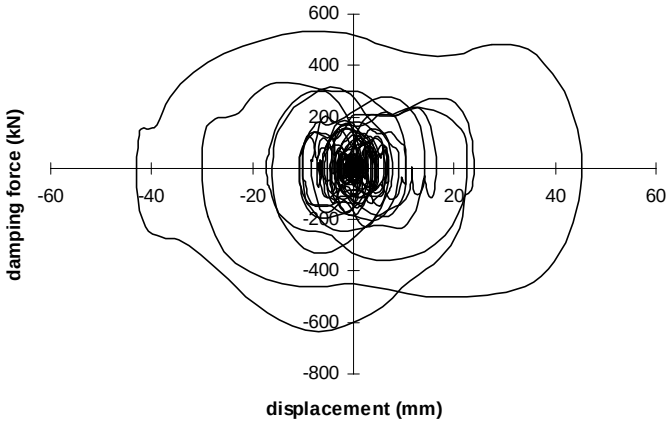

Figure 8 Damping Force-Displacement Loop at Middle Bearing (Northridge)

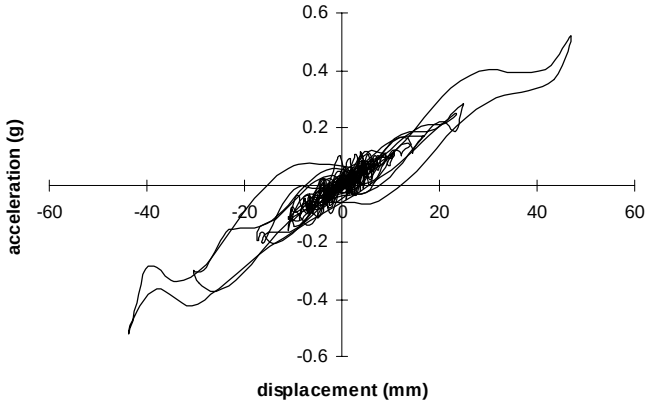

Figure 9 Damping Force-Displacement Loop at Middle Bearing (Northridge)

The damping ratio is increased by placing two fluid dampers at each bearing. The reduction in response is minimal when the number of dampers was doubled. The fluid damping ratio for this case is 19.35%. Therefore, to reduce the response by adding more fluid dampers to the system is almost of no use when damping ratio has reached a certain value. The reduction of responses cannot be solely achieved by dampers.

The analysis for the case of the El Centro vertical component leads to similar phenomena. The only difference is that the maximum responses are less significant due to the smaller peak ground acceleration. The maximum undamped response of displacement at mid-span is $23.7\,mm$ $(0.93\,in)$ and the acceleration is $0.240\,g$. The response of displacement, velocity and acceleration for the case with one damper placed at each bearing decreases by 49.8%, 50.7%,

and 42.1%, respectively, where the fluid damping level is 13.3%. When two dampers were used at each bearing, the response of displacement and velocity at mid-bearing had minimal reduction while the acceleration at mid-bearing slightly increased. This result is expected, since damping is effective in reducing the displacement. As a trade-off, the response of the acceleration would increase with a decrease in displacement.

As mentioned previously, damping is more efficient in reducing the displacement of an undamped system. For the damped system, using more than one damper decreases the response of displacement very little and even increases the response of acceleration. Therefore, to achieve an ideal effect one can use a more flexible system such as helical springs in combination with dampers to reduce the response.

Of particular interest is the response at the mid-span of the bridge subjected to vertical earthquake ground motion. Conventional bearings have too much stiffness in the vertical direction and cannot resist vertical motion. The vertical response of acceleration at mid-span would be significant, especially in the event of the Northridge earthquake with its large vertical ground acceleration. The spring bearings show the promise of providing the flexibility needed in the vertical direction.

Next, to show the isolation effects of the spring bearing, the isolated and non-isolated responses at the center bearing and at the mid-span of bridge model subjected to Northridge and El Centro vertical ground acceleration are compared in Table 2. In the non-isolated case, the bridge girder becomes flexible relative to the rigid supports. There is a significant difference between the response of acceleration at the bearing and at the mid-span. For the non-isolated case, the response of the acceleration can be over 2g for the bridge when subjected to a strong ground motion such as the Northridge earthquake. In addition, the maximum acceleration at mid-span is also larger than the undamped isolated acceleration response. Even in the event of an earthquake with small peak vertical ground acceleration, such as El Centro, the acceleration at the bearing is as low as 0.2 g while the acceleration at the mid-span is over 0.5 g .

Table 2. Maximum Vertical Responses of Isolated and Non-Isolated Bridge Model

Equake	Location	Damping	Displacement (mm)	Velocity (mm/s)	Acceleration (g)	Fluid Damping (%)
Northridge	Bearing	isolated+undamped	76.3	700.4	0.749	0.00
		isolated+damped	45.2	546.0	0.541	9.16
		non-isolated	0.0	0.0	0.792	0.00
	Mid-span	isolated+undamped	78.6	727.9	0.796	0.00
		isolated+damped	46.8	555.3	0.523	9.16
		non-isolated	7.8	451.0	2.300	0.00
El Centro	Bearing	isolated+undamped	23.0	233.1	0.225	0.00
		isolated+damped	11.9	120.3	0.147	13.30
		non-isolated	0.0	0.0	0.208	0.00
	Mid-span	isolated+undamped	23.7	239.5	0.240	0.00
		isolated+damped	11.9	118.0	0.139	13.30
		non-isolated	1.9	127.9	0.560	0.00

Therefore, if the bridge is not flexible enough in the vertical plane, the response of acceleration can be greater than the ground acceleration, even though the response of displacement at mid-span is negligible. For the isolated undamped case, the acceleration responses are reduced over 50% at mid-span of the bridge compared to the non-isolated case for both earthquakes, resulting

in reduced inertia force on the bridge structure. The isolated damped case is of more practical significance as the response of displacement and velocity due to the increase in the flexibility from the isolation device can be reduced over 50%. This is done by the addition of over 10% damping ratio without causing over-damping as may be the case in a linear damped system.

For the isolated cases, the maximum response of acceleration throughout the bridge span is limited to $0.54\,g$ for Northridge and $0.2\,g$ for El Centro. Hence, the bridge is protected from vertical ground motion by introducing spring bearings which result in a more flexible bridge system. The large response of displacement due to spring flexibility can effectively be reduced by damping.

Fig.10 illustrates three cases of maximum vertical dynamic deflection shape throughout the bridge model occurring at the same time. It can be observed that the vertical deflection throughout the span length of isolated bridge model has less variation than the non-isolated one, and that the relative deflection is reduced which is likely to result in reduction of stresses.

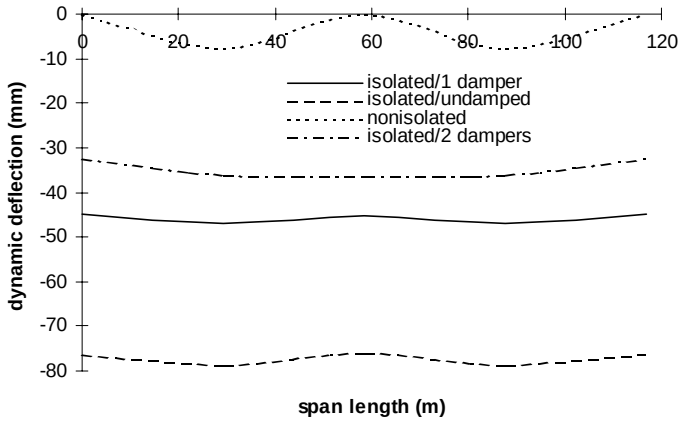

Figure 10. Vertical Deflection of Bridge Model Throughout Span

6. Conclusions

In order to achieve better protection for the bridge subjected to strong vertical ground motion, helical springs are used as bearings with fluid dampers as energy dissipators. The bridge model is supported on spring bearings in lieu of conventional rigid bearings. The spring-supported bridge is modeled to be much more flexible in the vertical direction. It is concluded that the response of acceleration in an isolated damped bridge model, particularly at the mid-span, has been greatly reduced up to 75% compared to the non-isolated case. Therefore, the inertia forces induced by acceleration response in the bridge structure are also reduced which in turn benefits the structural design. In addition, the damage from the deflection gap between the in-span and bearing is alleviated because of the flexibility due to the spring bearings.

The larger response of displacement of the bridge throughout the span, as a tradeoff of the flexible spring bearings, can be effectively reduced by adding fluid dampers to the isolation system. In general, bridge structures have damping levels less than 10% critical. The damping level of a structural system isolated by fluid dampers could be over 20% with more energy absorbed, offering a dramatic reduction in deflection at no cost of increase in base shear.

It is noted that extra damping becomes less efficient at higher damping levels. Reduction of response will hardly be achieved by only adding more dampers, especially in a less flexible bridge system. The stiff system is more sensitive to the ground acceleration excitation and the response of acceleration is greater than the flexible system. Use of helical springs as bearings

will certainly provide additional flexibility for the bridge structural system in which the displacements are controlled by dampers. The proposed bridge system is effective in greatly reducing the structural responses and relative deflection.

Acknowledgments

Financial support of this project has been provided by the National Science Foundation, Grant No. CMS-9502772. All earthquake ground motion records were made available from the University of Southern California via World Wide Web, and from the University of California at Berkeley via Gopher.

REFERENCES

1. Papazoglou, A.J., and Elnashai, A.S. 1996. Analytical and Field Evidence of the Damaging Effect of Vertical Earthquake Ground Motion. Earthquake Engineering and Structural Dynamics, **25**: 1109-1137.
2. Button, M.R. Cronin, C.J., and Mayes, R.L. 1999. Effect of Vertical Ground Motions on the Structural Response of Highway Bridges. Multidisciplinary Center for Earthquake Engineering Research Report 99-0007, State University of New York at Buffalo, Buffalo, NY.
3. Waisman, F., and Grigoriu, M. 1994. Effectiveness of Vibration Isolation Systems for Bridges. Proceedings of the First World Conference on Structural Control. Los Angeles, CA, Vol.1, pp. 30-39.
4. Saadeghvaziri, M., and Foutch, D.A. 1991. Dynamic Behavior of R/C Highway Bridges Under the Combined Effect of Vertical and Horizontal Earthquake Motions. Earthquake Engineering and Structural Dynamics, **20**: 535-549.
5. Xue, S., Kurita, S., and Tobita, J. 1997. Mechanics and Dynamics of Intelligent Passive Vibration Control System. Journal of engineering Mechanics **123**:323-327.
6. Nagarajaiah, S., Reinhorn, A., and Riley, M.A. 1993. Control of Sliding-Isolated Bridge with Absolute acceleration Feedback. Journal of engineering Mechanics, **119**: 2317-2332.
7. Yang, J.N., Kawashima, K., and Wu, J.C. 1995. Hybrid Control of Seismic-Excited Bridge Structures. Earthquake Engineering and Structural Dynamics, **24**:1437-1451.
8. GERB Schwingungsisolierungen GmbH&Co., KG. 1994. Vibration Isolation Systems. 9th Edition, Berlin, Germany.
9. Hueffmann, G.K. 1991. Protection of Spring Supported Equipment Against Seismic Excitation. Seismic, Shock, and Vibration Isolation, PVP, **222**: 45-50.
10. Waller, R.A. 1969. Building on Springs. Pergamon Press, UK.
11. Taylor, D.P., and.Constantinou, M.C. 1995. Testing Procedures for High Output Fluid Viscous Dampers Used in Building and Bridge Structures to Dissipate Seismic Energy. Shock and Vibration, **2**: 373-381.
12. Constantinou, M.C., Soong, T.T., and Dargush, G.F. 1998. Passive Energy Dissipation Systems for Structural Design and Retrofit. Multidisciplinary Center for Earthquake Engineering research Monograph No. 1, State University of New York at Buffalo, Buffalo, NY.
13. Soong T.T., and Constantinou M.C. 1994. Passive and Active Structural Vibration Control in Civil Engineering, Springer Verlag, Wien-New York.
14. Makris, N., Constantinou, M.C., and Hueffmann, G.K. 1991. Testing and Modeling of Viscous Dampers. Seismic, Shock, and Vibration Isolation, PVP, **222**: 51-56.
15. Clough, R.W., and Penzien, J. 1993. Dynamics of Structures. 2nd Edition, McGraw-Hill, New York.
16. Azar, J.J. 1972. Matrix Structural Analysis. Pergamon Press, UK.
17. Weaver, W., and Gere, J.M. 1990. Matrix Analysis of Framed Structures. Third Edition, Van Nostrand Reinhold, New York.
18. Delis, E.A., Malla, R.B., Madani M., and Thompson, K. J. 1996. Energy Dissipation Devices in Bridges Using Hydraulic Dampers. Proceedings of Structures Congress XIV, ASCE, Chicago, IL, Vol. 2, pp.1188-1196.
19. Nagarajaiah, S., Reinhorn, A.M., and Constantinou, M.C. 1991. 3D-Basis Nonlinear Dynamic Analysis of Three-Dimensional Base Isolated Structures: Part II. Multidisciplinary Center for Earthquake Engineering Research Report 91-0005, State University of New York at Buffalo, Buffalo, NY.

